Wind and Structures, *Vol. 30, No. 2 (2020) 199-210*
DOI: https://doi.org/10.12989/was.2020.30.2.199

Natural wind impact analysis of transiting test method to measure wind pressure coefficients

Lulu Liu[1,2a], Shengli Li[*1,2], Pan Guo[1,2] and Xidong Wang[1,2c]

[1]*School of Civil Engineering, Zhengzhou University, Zhengzhou, China*
[2]*Zhengzhou Key Laboratory of Disaster Prevention and Control for Cable Structure, China*

(Received March 14, 2018, Revised July 28, 2019, Accepted September 15, 2019)

Abstract. Building wind pressure coefficient transiting test is a new method to test the building wind pressure coefficient by using the wind generated by a moving vehicle, which is susceptible to natural wind and other factors. In this paper, the Commonwealth Advisory Aeronautical Research Council standard model with a scale ratio of 1:300 is used as the test object, and the wind pressure coefficient transiting test is repeated under different natural wind conditions to study the influence of natural wind. Natural wind is measured by an ultrasonic anemometer at a fixed location. All building wind pressure coefficient transiting tests meet the test conditions, and the vehicle's driving speed is 72 km/h. The mean wind pressure coefficient, the fluctuating wind pressure coefficient, and the correlation coefficient of wind pressure are used to describe the influence of natural wind on the building wind pressure coefficient transiting test qualitatively and quantitatively. Some rules, which can also help subsequent transiting tests, are also summarized.

Keywords: transiting test method; moving vehicle; natural wind; CAARC; wind pressure coefficient; ultrasonic anemometer; Reynolds number effect

1. Introduction

The building wind pressure coefficient is an important parameter in the study of wind resistance on buildings (Feng *et al.* 2018, Liu *et al.* 2011). Moreover, it is of utter importance to study wind effects on high-rise and low-rise buildings (Wang and Li 2015, Yuan *et al.* 2018). At present, the most commonly used methods in studying the wind pressure coefficient of buildings are the wind tunnel test (Kim *et al.* 2018, Alminhana *et al.* 2018, Bhattacharyya *et al.* 2018, Rizzo and Ricciardelli 2017), Computational Fluid Dynamics (CFD) (Yu *et al.* 2015, Montazeri and Blocken 2013, Cheng *et al.* 2017), and full-scale field measurement research (Dalgliesh 1975, Zhang *et al.* 2018, Yi *et al.* 2015). The Commonwealth Advisory Aeronautical Research Council (CAARC) standard high-rise building model is a hexagonal geometric test building model (Alminhana *et al.* 2018), that is widely used in wind tunnel test (Dalgliesh *et al.* 1975, Melbourne 1980) and CFD numerical simulation wind field methods (Yan 2015, Daniels *et al.*, 2013) to verify and calibrate the reliability of results. In previous works, a new test method was proposed to test the building wind pressure coefficient by using the wind generated by a moving vehicle (Wu 2018), which provides new attempts and options for structural wind resistance research (Guo *et al.* 2019). The test platform, software, and hardware system were designed for the building wind pressure coefficient transiting test. The test was carried out with the CAARC standard model, and the test results have the same trend as the wind tunnel test results, which verify the feasibility of the transiting test under ideal conditions.

For wind tunnel test, CFD, and field measurement, these three research methods of structural wind resistance have their own shortcomings. Such as, CFD is characterized by low cost and flow visualization but it is usually limited by grid size and mathematical model (Daniels *et al.* 2013, Meng *et al.* 2018). There is no adequate mathematical model of turbulent flows, and we cannot solve completely the problem of aerodynamic designing by numerical simulation (Rašuo 2006, Argentini *et al.* 2016). Field measurement is the most practical measurement method, but it is also usually limited by meteorology and topography, such as the establishment of structural health monitoring (SHM) (Wang *et al.* 2019) systems and wind pressures of high skyscraper (Zhang *et al.* 2018). The wind tunnel test is the most common experimental method, however, the establishment of exact two-dimensional flow conditions in wind tunnels is a very difficult problem (Rasuo 2012, Ocokoljić 2018). it is usually affected by the blocking effect (Marta *et al.* 2016, Huang 2014) Reynolds number effect (Rašuo 2011), the wall interference and supporting system interference, (Ocokoljić *et al.* 2017). Because of the scale model in the wind tunnel test, it will be affected by the Reynolds number effect. Rašuo has done some wind tunnel tests to study the influence of reynolds number, side-wall boundary-layer control and wall on the accuracy of the lift coefficient of the aerofoil NACA0012.

*Corresponding author, Assistant Professor
E-mail: lsl2009@126.com
[a]M.A. Student
E-mail: 643626951@qq.com
[b]Ph.D.
E-mail: 77741289@qq.com
[c]Ph.D.
E-mail: xidong.wang@zzu.edu.cn

ISSN: 1226-6116 (Print), 1598-6225 (Online)

In addition, Lj.Linić et al (2018) and Rašuo (2001) also study the boundary-layer transition in the wind tunnel to improve the accuracy of the wind tunnel text. Many scholars are working hard to improve the wind tunnel test method (Rašuo 2006, He *et al.* 2017).

Transiting test, as a new attempt and option for structural wind resistance research, is not only for studying building wind pressure coefficients, but also for other wind resistance research and practical applications, such as, the aerodynamic coefficient of structures (Li *et al.* 2019), galloping of iced conductor (Guo *et al.* 2019) and aerodynamic performance of wind turbine and wind turbine airfoil. However, transiting test also are affected by some influences, such as, end plate, road types (Li *et al.* 2019), reynolds number and natural wind. These factors, which are the source of inaccuracy of tests are our key research object to improve the exactness of transiting test. Natural wind is the main disturbance factor of the outside environment. Further studies about natural wind must be conducted. Investigating the effects of natural wind on the transiting test results that consider CAARC standard model as research objects is significant, thereby providing references for the weather condition used for transiting tests and providing suggestions and guidance for subsequent building wind pressure coefficient transiting tests qualitatively and quantitatively.

In addition, Natural wind is a random variable in which airflow and terrain roughness work together on time and space scales (Li 2016). Outdoor tests are inevitably affected by natural wind. Many outdoor experimental studies must consider the effects of natural wind. For example, the random wind impact analysis of the safety of high-speed trains (Yu *et al.* 2016, Baker *et al.* 2010), indoor ventilation research (Liang *et al.* 2011), analysis of the influence of natural wind on vehicle aerodynamic coasting down test (Altinisik 2017, McAuliffe *et al.* 2016), and vehicle safety study must consider the influence of crosswind (Wang *et al.*2017). Yu *et al.* (2016) studied the effect of natural wind on the safety of high-speed trains by applying natural wind on high-speed trains with CFD. Wang *et al.* (2017) also studied the safety of road vehicles under random variables, such as crosswinds by CFD numerical simulation. McAuliffe *et al.* (2016) placed a 3D ultrasonic anemometer at a height of 2 m on both sides of a vehicle's taxi track to measure the natural wind speed when testing the aerodynamic performance of the heavy-duty passenger car, and concluded that natural wind effect should be considered when analyzing pulsating wind speed data. José Páscoa *et al.* (2012) considered that the windless condition test is accurate when performing vehicle aerodynamic performance coasting down test and found after repeated tests that 4% of the test error is mainly caused by natural wind. Zhang *et al.* (2017) designed a virtual test system for vehicle road sliding resistance and realized compensation for natural wind, thereby reducing natural wind impact and improving test accuracy. The vehicle aerodynamic coasting down test specification (SAE, J1263) specifies that the surrounding natural wind should be <2 m/s during the test. Therefore, according to the feasibility of the transiting test under ideal conditions, the analysis of the influencing factors with natural wind as a single variable is important in verifying the general applicability of the transiting test and improving its accuracy.

Natural winds can affect the effective wind field generated by the moving vehicle. Under ideal conditions, the wind field generated by the moving vehicle at a constant speed can be regarded as the quasi-steady uniform flow. Comparing the wind tunnel test to simulate the boundary layer wind tunnel on the basis of uniform flow field (Alminhana *et al.* 2018) showed that the ultimate goal of the building wind pressure coefficient transiting test is to imitate the atmospheric boundary layer on the basis of uniform and stable vehicle wind field, and natural wind affects the stability of wind field uniformity (McAuliffe *et al.* 2014, Wordley *et al.* 2008). McAuliffe *et al.* (2014) installed multiple cobra probes in the front of the car to study the wind turbulence of the car at a constant speed cruise and compared the influence of traffic, road conditions, and natural wind. Wordley *et al.* (2008) showed that the turbulence of wind field generated by a constantly moving vehicle is approximately 4%, and it is easily disturbed by the surrounding environment.

The building wind pressure coefficient transiting test is a new test method, and no scholars have conducted natural wind impact analysis and research to date. Therefore, the influencing factors of natural wind should be analyzed. In this paper, the building wind pressure coefficient transiting test is carried out with CAARC standard high-rise building model as the test object under different natural wind conditions to study how natural wind affects the wind pressure coefficient. The effects of natural wind on the surface mean wind pressure coefficient and fluctuating wind pressure coefficient of CAARC model are analyzed qualitatively and quantitatively. Lastly, some rules are summarized to provide suggestions and guidance for subsequent building wind pressure coefficient transiting tests.

2. Experimental

2.1 Transiting test and model introduction

The building wind pressure coefficient transiting test is a transiting test method that uses wind generated by a moving vehicle to test the wind pressure coefficient of the model (Wu 2018). As shown in Figs. 1 and 2, the building wind pressure coefficient transiting test devices are mainly composed of an external test platform and an interior collecting instrument and system. The external test platform is used to fix test models and pitot tube (Fig. 1), The in-vehicle acquisition system includes a multipoint, a high-frequency dynamic wind pressure synchronous measurement system, and a pitot tube wind speed measurement system, which consists of 22 high frequency pressure sensors (YMC41-D), a multichannel USB data acquisition card (USB2805C), a 24 V power supply, and a notebook computer (Fig. 2). Twenty pressure sensors are connected to the CAARC standard model surface measuring point through the PVC hose to obtain surface

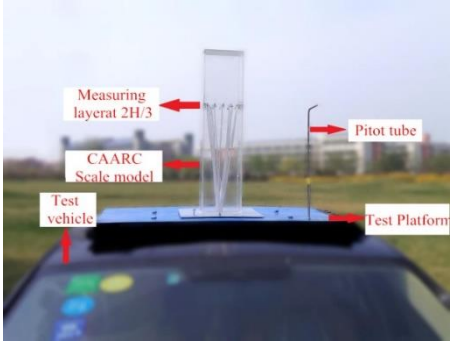

Fig. 1 External test platform of transiting test

Fig. 2 Interior collecting instrument and system arrangement

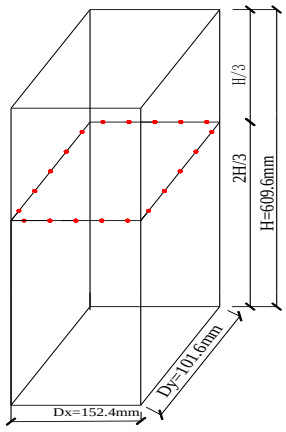

Fig. 3 Dimensions and shape of CAARC standard model

wind pressure, and two pressure sensors are connected to the total and static pressure holes of the pitot tube to obtain the driving wind field characteristics. The static pressure of the pitot tube can be used as a reference static pressure for the dimensionless wind pressure coefficient. In this test, the sampling frequency was 1000 Hz, and the number of data points acquired in each channel was 30000.

The CAARC rigid model in the transiting test used a 1:300 geometric scale ratio (Alminhana *et al.* 2018), whose dimension is 152.4 mm × 101.6 mm × 609.6 mm (Fig. 3). The model was made of 5 mm thick Plexiglas that was bonded together with a chloroform reagent. The bonding ensured sufficient model strength and stiffness. Generally, 20 measuring points were arranged at the height of the model 2/3 *H* as the standard pressure measuring point. As

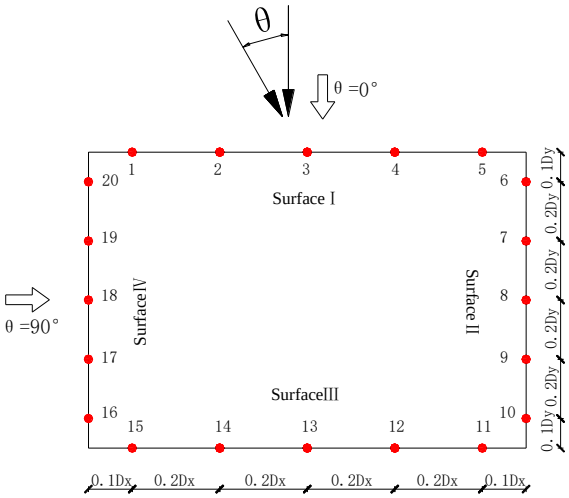

Fig. 4 Measuring point at the height of 2H/3

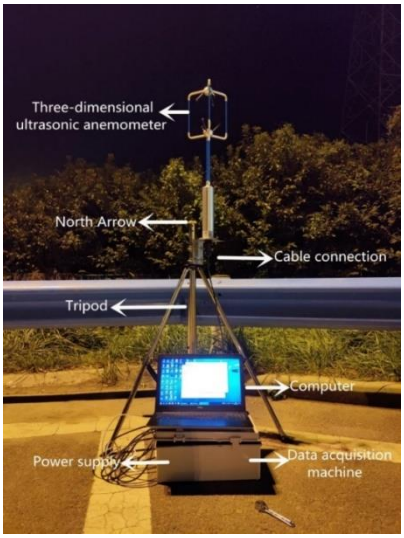

Fig. 5 Natural wind collection system

shown in Fig. 4, surfaces I - IV represented the four surfaces of the model, and θ represented the windward angle of the model, which was positive in counter-clockwise rotation.

2.2 Natural wind measurement

Natural wind is a space vector (Li 2016) that can be measured by a 3D ultrasonic anemometer (Van *et al.* 2015, Fiedler *et al.* 2013). As shown in Fig. 5, the natural wind collection system test was composed of a 3D ultrasonic anemometer (Wind Master, Gill Scientific Inc., Logan UT), a data acquisition instrument (CR1000, Campbell Scientific Inc., Logan, UK), and a notebook computer. The natural wind collecting device was assembled and installed at a height of 1.5 m at the fixed measuring location of the test. The 0° line of the anemometer points to the north, which was determined by using the north arrow. The sampling frequency was set to 10 Hz, and the wind speed resolution is 0.01 m/s. The natural wind data acquisition was synchronized with the transiting test wind pressure

measurement, and the natural wind here was used as a reference standard of natural wind conditions.

2.3 Test methods and strategies

Natural wind impact analysis test, which measures the wind pressure coefficients by using the wind generated by a moving vehicle, needs to be combined with the wind pressure test and natural wind collecting systems. Observing the natural wind while conducting a transiting test, the test procedure is shown in Fig. 6. A straight route from point A of Zhongyuan West Road Station to Point B of Yulong Station in China Zhengzhou G3001 Ring Expressway was selected as the test route of the transiting test, which is 2 km long (Fig. 7). The text route is straight, and few bushes grow on both sides of the road from the beginning to the end. The test road conditions are shown in Fig. 8. The selected test time was at night when the traffic is light. The natural wind measuring point was fixed at the outer space of the original point A at Zhongyuan West Road Station, which is close to the high-speed way, and the surrounding terrain environment was consistent with the test road conditions. The natural wind at the measuring point was assumed to be equivalent to the natural wind during the test.

To obtain different natural wind conditions, we carried out tests under different weather conditions on different dates in October. Meanwhile, to keep other conditions, except natural wind, consistent, we carried out tests in the same test route, and natural wind measurement points remained unchanged. The speed of 72 km/h was selected as the test speed of the moving vehicle, and 19:00 - 20:00 was selected as the test time when the traffic volume is light. The natural wind data were recorded during the transiting test; when the test speed was stable at 72 km/h, the wind pressure data was recorded. The sampling time was 30s, and the number of tests was 3. The test conditions are shown in Table 1. Two typical CAARC standard model wind direction angles of 0° and 90° were chosen as the test condition, which can guarantee the credibility of the natural wind impact analysis results. Test route takes a round trip, and sets A–B and B–A, that is, the down- and headwind directions, can be used to study the influence of downwind and headwind. Among the test routes, Zhongyuan West Road Station travelled to Yulong Station with A–B, and Yulong Station to Zhongyuan West Road Station was indicated by B - A (Table 1). The speed of natural wind was mainly in the range of 0 - 2.0 m/s, and detailed data processing and analysis of natural wind condition are shown in section 3.3.

Table 1 Test conditions

Test speed	Wind direction angle	Test route	Natural wind V(*nw*)
72 km/h (20 m/s)	0°	A–B	0–2.0 m/s
		B–A	0–2.0 m/s
	90°	A–B	0–2.0 m/s
		B–A	0–2.0 m/s

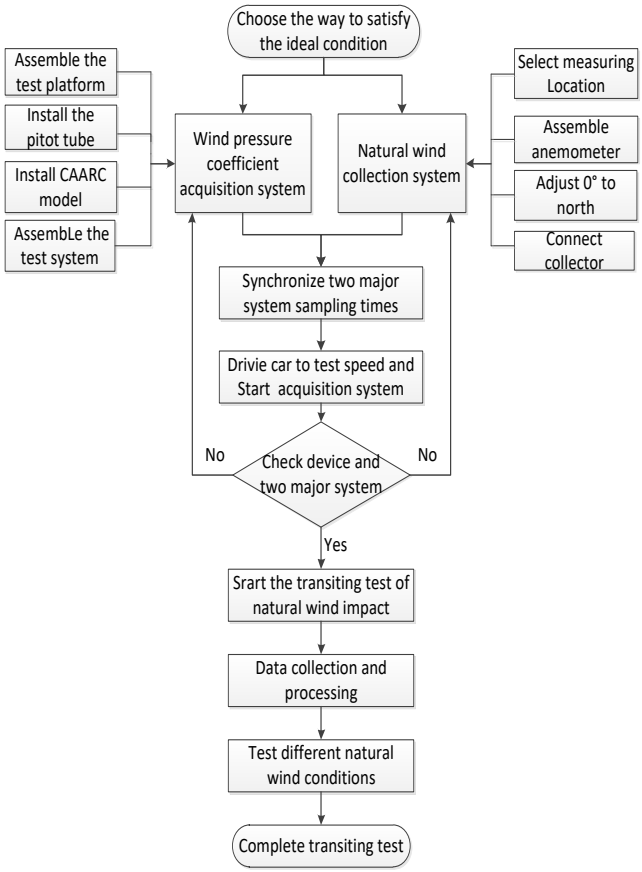

Fig. 6 Transiting test procedure

Fig. 7 Test route

3. Data processing

3.1 Wind pressure coefficient data processing

According to the wind tunnel test, the wind pressure coefficient can be written as follows (Zou *et al.* 2015)

$$C_{pi}(t) = \frac{P_i(t) - P_0(t)}{\frac{1}{2}\rho U^2}, \quad (1)$$

where $P_i(t)$ is the pressure value of the measuring point; $P_0(t)$ is the static pressure value of the incoming flow; U is the average wind speed of the incoming flow; ρ is the air

Fig. 8 Test road conditions

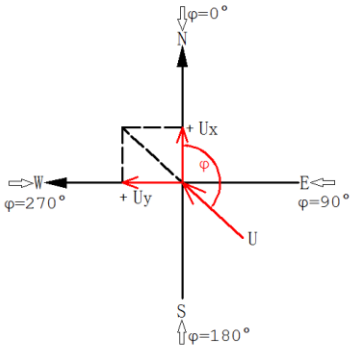

Fig. 9 Wind speed coordinate system

Table 2 Natural wind conditions

Working condition	Test date	Natural wind speed (m/s)	Natural wind direction
1	2018/10/16	0.22±0.05	100°±26°
2	2018/10/25	0.56±0.17	284°±17°
3	2018/10/28	1.20±0.80	267°±50°

density, whose value is 1.225 kg/m^3; and $C_{pi}(t)$ is the wind pressure coefficient of the measuring point.

Pitot tube and pressure sensors are used to test the wind speed directly. Pitot tube and pressure sensors are also used to measure the total and static pressures, and the wind speed can be calculated based on the Bernoulli equation, as follows (Chevula *et al.* 2015)

$$V_{mean} = U = \sqrt{\frac{2(P_p(t)-P_0(t))}{\rho}}, \quad (2)$$

The wind pressure coefficient expression can be simplified to the following

$$C_{pi}(t) = \frac{P_i(t)-P_0(t)}{P_p(t)-P_0(t)}, \quad (3)$$

The mean wind pressure coefficient is expressed as follows

$$C_{pi,mean} = \frac{1}{T}\int_0^T C_{pi}(t)dt, \quad (4)$$

The fluctuating wind pressure coefficient is expressed as follows (Liu *et al.* 2013, Zou *et al.* 2015)

$$C_{pi,flu} = \sqrt{\frac{1}{N-1}\sum_{k=1}^{N}(C_{pik} - C_{pi,mean})^2} \quad (5)$$

where $C_{pi,mean}$ is the value of mean wind pressure coefficient, $C_{pi,flu}$ is the value of fluctuating wind pressure coefficient, $P_0(t)$ is the static pressure value at the reference height, $P_p(t)$ is the total pressure value at the reference height, $P_i(t)$ is the wind pressure value of the measuring point, T is the sampling time, and N the number of samples.

3.2 Natural wind data processing

The 3D ultrasonic anemometer is fixed at the wind measurement point to record the surrounding natural wind speed. The natural wind can be regarded as a 3D vector, in which the three components can be expressed in a north–south direction $U_X(t)$, east–west direction $U_Y(t)$, and vertical direction $U_Z(t)$. The wind angle of the natural wind in the vertical direction is extremely small, and the wind direction is consistent with the horizontal direction (Li 2016). Thus, $U_Z(t)$ is negligible. The natural wind velocity $V(nw)$ of the horizontal wind direction angle φ is expressed as follows (Li 2016)

$$V(nw) = \sqrt{U_X^2+U_Y^2}, \quad (6)$$

$$\varphi = Degree(-\arccos\left(\frac{U_X}{U}\right) * sgn(U_Y)) + 180°, \quad (7)$$

As shown in Fig. 9, to describe the natural wind direction, we superimpose the coordinate system of the anemometer with the geographic coordinate system, that is, the 0 scale of the anemometer points to the north, and natural wind is analyzed with the basic wind speed of 10 minutes (Li 2016).

3.3 Natural wind data statistics

Figs. 10(a) - 10(c) show the wind speed distribution and wind rose diagram of the surrounding natural winds during the transiting tests which are carried out at three different natural wind conditions. The three natural wind time history curves are shown in Fig. 10(d). The main direction of the natural wind is west, and the main wind speed is between 0 and 2 m/s. As shown in Table 2, the mean values of natural wind speeds corresponding to the three working conditions are 0.22, 0.56 and 1.20 m/s.

4. Results and discussion

4.1 Influence of natural wind on driving wind of moving vehicle

Natural wind with nonstationary characteristics is the airflow caused by the interaction of atmospheric motion and surface roughness (Li 2016). Thus, natural wind may affect the effective wind field generated by the moving vehicle. Pitot tube and pressure sensors are used to measure the total and static pressures, and the wind speed can be calculated based on the Bernoulli equation Eq. (2). The speed of the moving vehicle is fixed at 72 km/h (20 m/s) by using a fixed speed cruise, and the sampling time is 30 s.

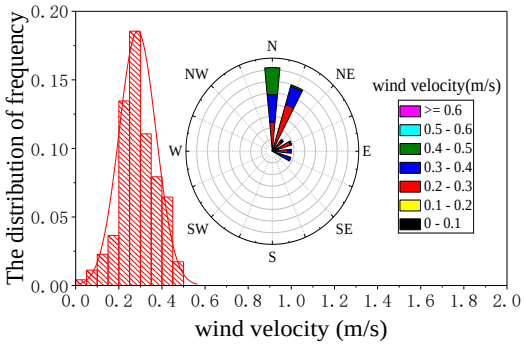

(a) V(nw)=0.22±0.05 m/s

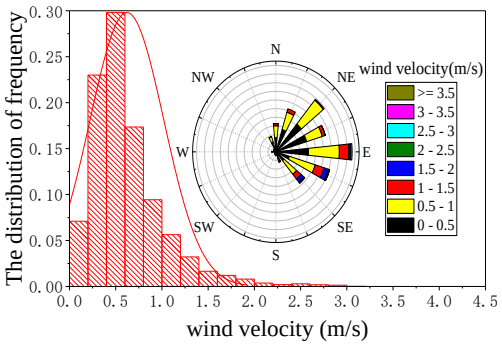

(b) V(nw)=0.56±0.17 m/s

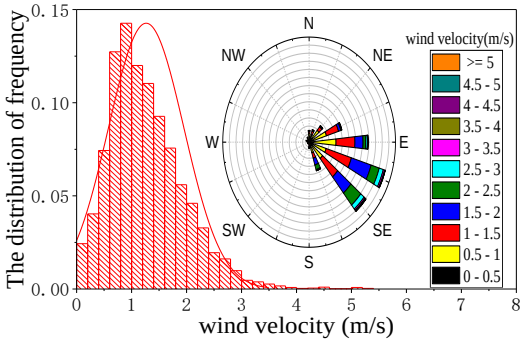

(c) V(nw)=1.20±0.80 m/s

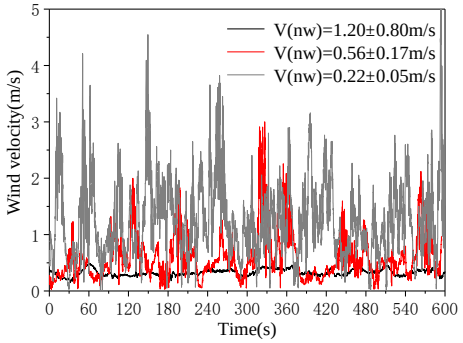

(d) Graphs of natural wind time history curve

Fig. 10 (a) - (c) Graphs of natural wind rose, (d) graphs of natural wind time history curve

As shown in Figs. 11 and 12, comparing the time history diagram and the distribution histogram of driving wind of the moving vehicle under different natural wind shows that in the range of 0 - 1.20 m/s of natural wind speed, the natural wind increases, the wind speed time history curve declines, and the wind speed time history curve becomes disordered. The wind speed variation coefficient can be used to describe the degree of variation with time and space. The value is the ratio of the mean square error of the wind speed pulsation component to the average wind speed, which can be expressed as follows

$$I_V = \frac{\sigma}{V_{mean}}, \tag{8}$$

The results are shown in Table 3, when the speed of natural wind increases from 0.22 m/s to 1.20 m/s, the coefficient of variation of the driving wind field of the moving vehicle is also increased from 0.05 to 0.11. Therefore, natural wind will disturb the turbulence characteristics of the driving wind of the moving vehicle, and the uniformity of the driving wind field will also deteriorate.

Table 3 Variation coefficient of moving vehicle driving wind

Natural wind velocity $V_{(nw)}$ (m/s)	Mean velocity of driving wind V_{mean} (m/s)	Driving wind standard deviation σ	Coefficient of variation I_V
0.22±0.05	18.22	0.91	0.05
0.56±0.17	17.41	1.03	0.06
1.20±0.80	18.19	2.01	0.11

4.2 Comparative analysis of down- and headwind

Although natural wind is nonstationary, its main wind direction does not change significantly (Li 2016). The difference in the driving direction of the transiting test will result in the difference between the down- and headwind direction tests due to the presence of natural wind. For example, in the 0° wind direction angle of the natural wind speed at 0.56 m/s, the main wind of natural wind is northwest. Combining with the test route (Fig. 7), the vehicle traveling from A to B is headwind, whereas the vehicle traveling from B to A is downwind. Table 4 compares the results under the down- and headwind conditions. The dynamic pressure values measured by the pitot tube in the headwind direction are less than the dynamic pressure measured in the downwind direction, and the influence of natural wind on the dynamic pressure value also exists.

As shown in Fig. 13, in terms of the comparison of the mean wind pressure coefficient under the condition of down- and headwind, the curves are completely consistent. The difference of wind pressure coefficient does not show a uniform regular pattern, and the absolute value of the difference is in the range of 0.05, which is negligible. Although down- and headwind conditions have effects on the dynamic pressure measured by the pitot tube, they have no effect on the mean wind pressure coefficient. Different driving directions essentially affect the speed of the measured wind of the driving vehicle, which is reflected by the dynamic pressure value of the pitot tube. However, the wind speed does not affect the average wind pressure coefficient of the CAARC surface. This result is consistent

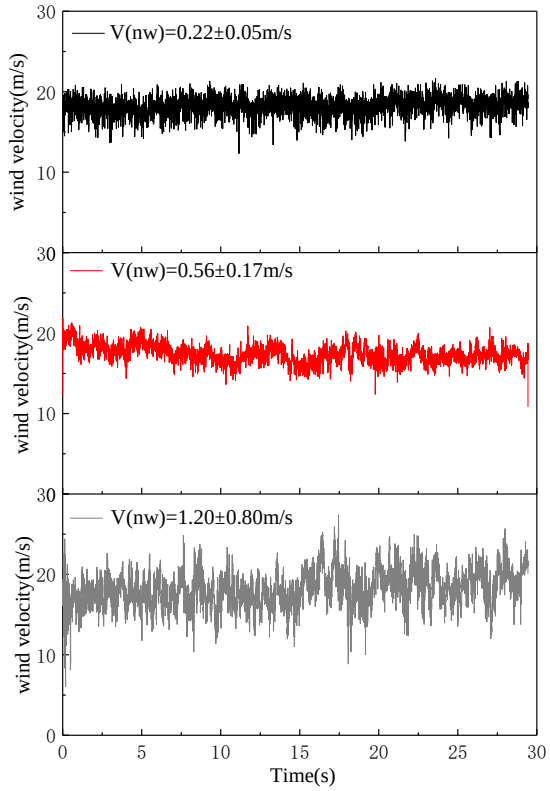

Fig. 11 Time history diagram of the wind generated by a moving vehicle under different natural wind conditions

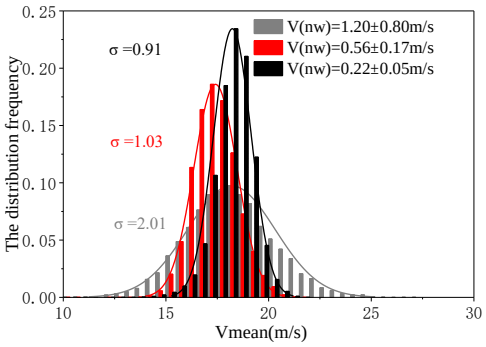

Fig. 12 Distribution histogram of speed of wind generated by a moving vehicle under different natural wind conditions

Table 4 Dynamic pressure values of in the downwind and headwind tests

Vehicle direction	Test	Dynamic pressure values measured by pitot tube
A–B (downwind)	1	212
	2	232
	3	237
B–A (headwind)	1	177
	2	171
	3	178

with the conclusion that wind speed does not affect the surface wind pressure coefficient both in numerical simulation and wind tunnel test studies (Liu *et al.* 2013).

Therefore, due to the influence of natural wind, the dynamic pressure of the pitot tube in the downwind test is less than that of the headwind test. However, the average wind pressure coefficient is unaffected

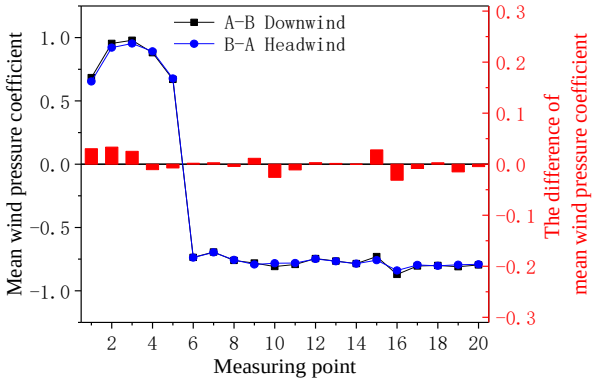

Fig. 13 Comparison between the mean wind pressure coefficients under the down- and headwind conditions

4.3 Influence of natural wind on mean wind pressure coefficient

The presence of natural wind directly affects the vehicle's driving wind field, which is reflected by the surface wind pressure coefficient of the CAARC model. The mean wind pressure coefficient of the transiting test method under the different natural wind conditions of 0° and 90° wind direction angles, are compared and supplemented with the CAARC wind tunnel test results from Zhejiang University (Meng 2018). As shown in Figs. 14 and 15, comparison shows that the wind pressure coefficient curves of the transiting test are consistent with the trend of the wind tunnel test result. The wind pressure on the crosswind surface agrees well, while the positive pressure on the windward side is extremely large, and the negative pressure on the leeward side is small. This phenomenon can be explained by the fact that the turbulence of the wind tunnel test is larger than that of the transiting test (Lee *et al.* 1975). However, under different natural wind conditions, the wind pressure coefficient curve of the transiting test is highly consistent. Natural wind has no effect on the mean wind pressure coefficient curve of the 2/3H height of the CAARC model obtained from the transiting test, which also indicates that the building wind pressure coefficient transiting test still has certain feasibility and repeatability in the general natural wind range of 0 - 1.2 m/s.

To analyze the effect of natural wind on the mean wind pressure coefficient further, we compare the mean wind pressure coefficient values of four typical measuring points (#3, #8, #13, #18) on surfaces I - IV at the wind direction angles of 0° and 90° quantitatively. As shown in Figs. 14 and 15, the mean wind pressure coefficient values of the typical measurement points obtained from the test are relatively consistent under different natural wind conditions of 0 - 1.20 m/s. The standard deviation of the average wind pressure coefficient of 6 tests is lower than 0.04, and the difference of wind pressure coefficient of each measuring point is <0.1. Therefore, natural wind has a minimal effect

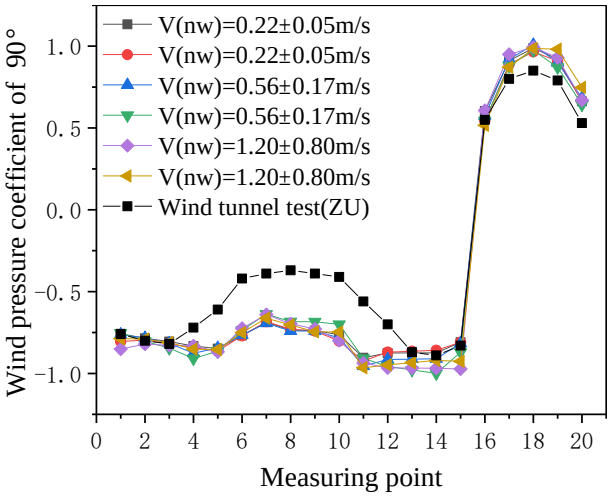

Fig. 14 Mean wind pressure coefficient curves under different natural wind conditions at 90° wind direction angle

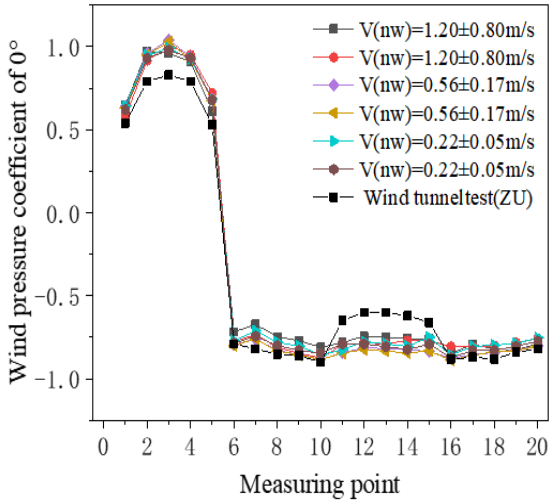

6

Fig. 15 Mean wind pressure coefficient curves under different natural wind conditions at 0° wind direction angle

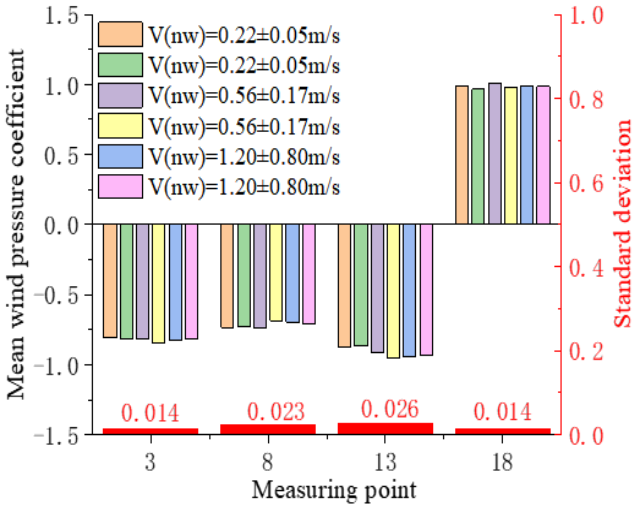

Fig. 16 Comparison of the mean wind pressure coefficient of typical measuring points at 90° wind direction angle under different natural wind conditions

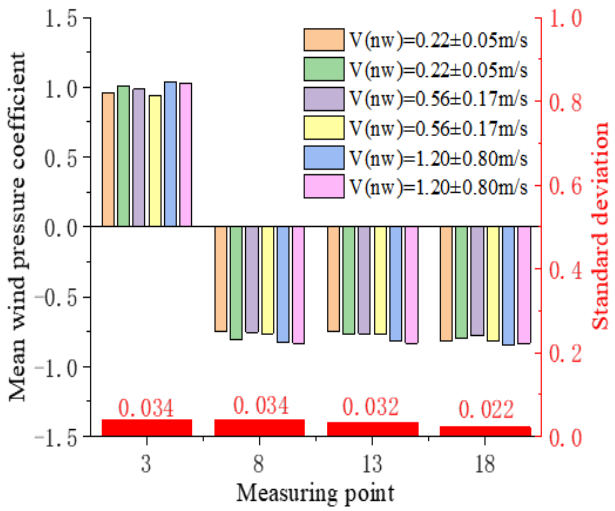

Fig. 17 Comparison of the mean wind pressure coefficient of typical measuring points at 0° wind direction angle under different natural wind conditions

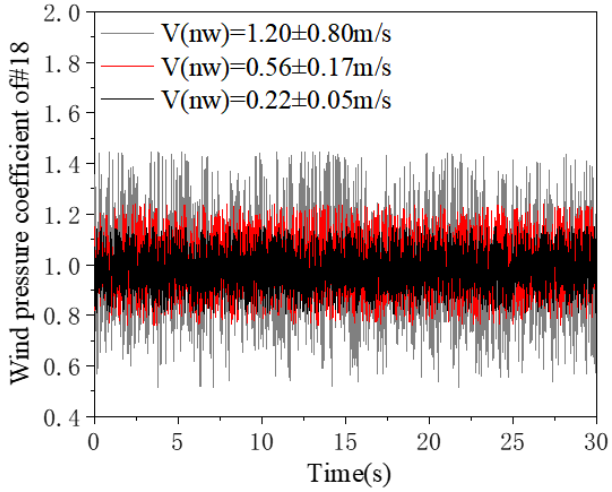

Fig. 18 Time history diagram of wind pressure coefficient of #18 measuring point at 90° wind direction angle under different natural wind conditions

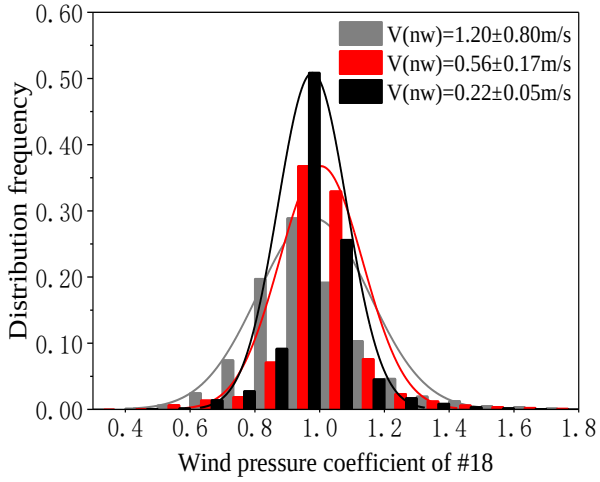

Fig. 19 Wind pressure coefficient distribution histogram of #18 measuring point at 90° wind direction angle under different natural wind conditions

on mean wind pressure coefficient in the range of 0 - 1.20 m/s, which is negligible.

As shown in Fig. 18, the wind pressure coefficient time history curve of the #18 measuring point at the 90° wind direction angle is selected for detailed analysis. As the natural wind speed increases in the range of 0 - 1.20 m/s, the fluctuation of the wind pressure coefficient becomes strong, and the data dispersion increases in size. As shown in Fig. 19, the distribution histogram also shows that the mean wind pressure coefficient is consistent, but the dispersion is extremely different when the natural wind speeds are 0.22, 0.56, and 1.20 m/s. Therefore, the influence of natural wind on the dispersion of the wind pressure coefficient cannot be ignored.

4.4 Influence of natural wind on fluctuating wind pressure coefficient

In section 4.3, the natural wind speed in the range of 0 - 1.20 m/s has no effect on the trend of the mean wind pressure coefficient curve, and the effect on the mean wind pressure coefficient is small and negligible. However, by analyzing the wind speed time history curve of the #18 measuring point of the windward surface at 90° wind angle (Figs. 18 and 19), the influence of natural wind on the dispersion of wind pressure coefficient data is evident. The degree of dispersion of the wind pressure can be reflected by the fluctuating wind pressure coefficient (Zou *et al.* 2015). In this section, the fluctuating wind pressure coefficient curves under different natural wind conditions are compared to study the influence of natural wind. Transiting test method results are also compared with the wind tunnel text from Zhejiang University (Meng 2018).

As shown in Fig. 20, at 0° wind direction angle, in the speed range of 0 - 1.20 m/s, natural wind does not affect the trend of the fluctuating wind pressure coefficient curves. The curves of the fluctuating wind pressure coefficient under different natural wind conditions of the transiting test method agree well, and all curves are similar to the trend of the wind tunnel results. However, the pulsating wind pressure coefficients under different natural wind conditions are relatively different. When the natural wind speed is 0.22 m/s, the fluctuating wind pressure coefficient of the transiting test is smaller than the wind tunnel test value. When the natural wind speed is 1.20 m/s, the fluctuating wind pressure coefficient is large. Except for the windward surface measuring point, the values of other measuring points are larger than those in the wind tunnel test. The difference in the pulsating wind pressure under different natural wind conditions is 0.22. Related studies have shown that an increase in turbulence also increases the fluctuating wind pressure coefficient (Cheng *et al.* 1992).

As shown in Fig. 21, at the 90° wind direction angle, in the range of 0 - 1.20 m/s, the curves of the fluctuating wind pressure coefficient under different natural wind pressures of the transiting test method also agree well, which is better than that of the 0° wind direction angle. Coincidentally, the fluctuating wind pressure coefficients under different natural wind conditions are significantly different. The difference is up to 0.26. When the natural wind speed is

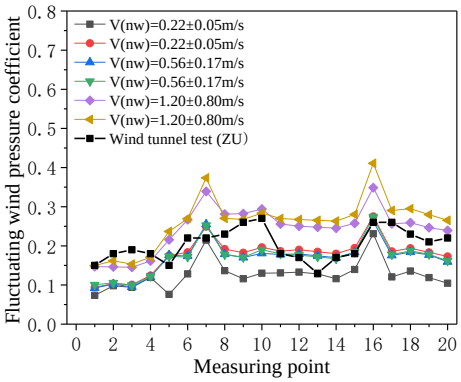

Fig. 20 Fluctuating wind pressure coefficient curves under different natural wind conditions at 0° wind direction angle

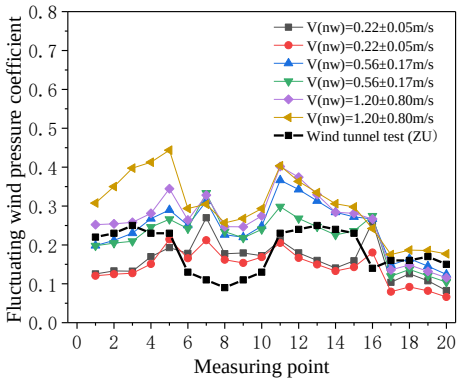

Fig. 21 Fluctuating wind pressure coefficient curves under different natural wind conditions at 90° wind direction angle

1.20 m/s, the maximum fluctuating wind pressure coefficient is 0.45, which is much larger than the fluctuating wind pressure coefficient of the natural wind speed of 0.22 m/s. The effect of natural wind on the fluctuating wind pressure coefficient is consistent at the 0° and 90° wind direction angles, which is credible.

Natural wind has no effect on the trend of fluctuating wind pressure coefficient curve in the range of 0 - 1.20 m/s but has an effect on fluctuating wind pressure coefficient. An increase in natural wind increases the fluctuating wind pressure coefficient. The difference in the fluctuating wind pressure coefficient under different natural wind conditions can reach 0.25, which cannot be ignored. Thus, the effect of natural wind on the fluctuating wind pressure coefficient is greater than that on the mean wind pressure coefficient.

4.5 Influence of natural wind on wind pressure correlation coefficient

Correlation coefficient is the statistic of the degree of linear correlation between two random variables in the time domain response. The wind pressure correlation coefficient is used to reflect the spatial correlation between CAARC standard model points. The correlation coefficient has a value in the range of [−1, 1]. The larger the absolute value is, the stronger the correlation is (Zhang *et. al* 2014). The formula is expressed as follows (Zhang *et. al* 2018)

$$Cor(i,j) = \frac{cov_{i,j}}{\sigma_i * \sigma_j} \quad , \tag{9}$$

where $Cor\ (i,j)$ denotes the two-point correlation coefficient of i-point and j-point; $cov_{i,j}$ denotes the covariance of i-point and j-point; σ_i denotes the standard deviation of the i-point wind pressure time history; and σ_j denotes the standard deviation of the j-point wind pressure time history.

As shown in Fig. 22, at the 0° wind angle, the #18 measuring point in surface IV was used as a reference point to calculate the correlation coefficient between all the measuring points of the height layer of 2H/3 and the reference point under different natural wind. The curve of the wind pressure correlation coefficient at each measuring point shows the same curve under different natural wind conditions. In the same plane of the reference point #18, the farther it is from the reference point, the smaller the correlation coefficient is, which is consistent with the wind tunnel test correlation analysis (Zhang *et. al* 2014). However, the correlation coefficient shows significant differences. The correlation coefficient has a large absolute value that is close to 1 when the natural wind speed is 0.22 m/s, while has a small absolute value that is close to 0 when the natural wind speed is 0.22 m/s.

As shown in Fig. 23, at the wind angle of 90°, the #3 measuring point at surface I was used as a reference point to calculate the correlation coefficient. Although the correlation curve of the 90° wind direction angle is inconsistent in the 0° wind direction angle, the natural wind condition corresponding to the worst correlation curve is still 1.20 m/s. The natural wind affects the synchronism between the measured points of the pulsating wind pressure, which decreases the correlation of the pulsating wind pressure time history and even affects the accuracy of the wind pressure coefficient.

Natural wind has an effect on the correlation coefficient of wind pressure in the range of 0 - 1.20 m/s. With the increase in natural wind, the correlation of wind pressure coefficient decreases. The correlation of wind pressure coefficient with $V_{(nw)}$ =1.20 m/s is substantially lesser than the others. Therefore, the building wind pressure coefficient transiting test should be carried out when the natural wind is <1.20 m/s after meeting the other test requirements.

5. Conclusions

In this study, considering the impact of environmental factors on the accuracy of building wind pressure coefficient transiting tests, it is essential to study the influence of natural wind and conduct transiting tests at a constant speed of 72 km/h under different natural wind conditions. The influence of natural wind in the range of 0–1.20 m/s on the wind pressure coefficient performance of CAARC standard model was investigated.

Natural wind disturbed the turbulence characteristics of the wind field of the vehicle, and the wind field uniformity deteriorated. When the mean velocity of natural wind was

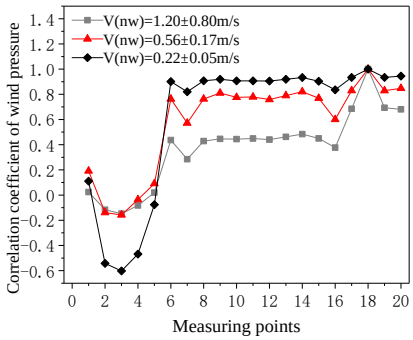

Fig. 22 Wind pressure correlation coefficient under different natural wind conditions at 0° wind direction angle

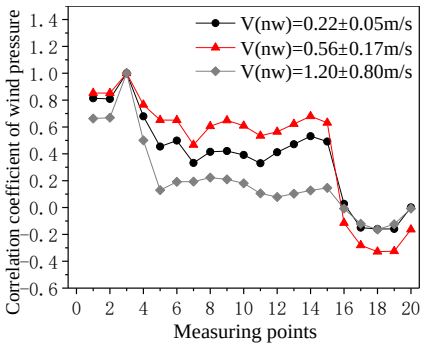

Fig. 23 Wind pressure correlation coefficient under different natural wind conditions at 90° wind direction angle

1.20 m/s, the coefficient of variation of the wind field reached 0.11. Considering the influence of natural wind, the dynamic pressure of the pitot tube under the downwind test was less than that of the headwind test. However, the average wind pressure coefficient was unaffected. When the mean velocity of natural wind is in the range of 0 - 1.20 m/s, natural wind had no effect on the trend of mean wind pressure coefficient curve and fluctuating wind pressure coefficient curve, and natural wind had a minimal effect on mean wind pressure coefficient, whose test error was within 0.1, which was negligible.

However, in the same situation, Natural had an effect on fluctuating wind pressure coefficient. An increase in natural wind increased the fluctuating wind pressure coefficient. The fluctuating wind pressure coefficient with $V_{(nw)}$ =1.20 m/s was significantly greater than those of the others. In addition, natural wind had an effect on the correlation coefficient of wind pressure in the range of 0 - 1.20 m/s. With the increase in natural wind, the correlation of wind pressure coefficient decreases. The correlation of wind pressure coefficient with $V_{(nw)}$ =1.20 m/s was significantly lower than the others. Therefore, it is recommended that the building wind pressure coefficient transiting test should be carried out when the natural wind was <1.20 m/s after meeting the other test requirements.

Acknowledgments

The authors are grateful for the financial support from

the National Natural Science Foundation of China (51778587, 51808510), Natural Science Foundation of Henan Province of China (162300410255), Supported by Foundation for University Young Key Teacher by Henan Province (2017GGJS005), Outstanding Young Talent Research Fund of Zhengzhou University (1421322059) and Science and technology planning project of Transportation in Henan Province (2016Y2-2, 2018J3), Key Scientific and Technological Research Projects of Henan Province (192102310514).

References

Alminhana, G.W., Braun A.L. and Loredo-Souza, A.M. (2018) "A numerical-experimental investigation on the aerodynamic performance of CAARC building models with geometric modifications", *J. Wind Eng. Ind. Aerod.*, **180**, 34-48. https://doi.org/10.1016/j.jweia.2018.07.001.

Altinisik, A. (2017), "Aerodynamic coast down analysis of a passenger car for various configurations", *Int. J. Automot Techn*, **18**(2), 245-254. https://doi.org/10.1007/s12239-017-0024-6.

Argentini T., Diana G., Rocchi D. and Somaschini C. (2016), "A case-study of double multi-modal bridge flutter: Experimental result and numerical analysis", *J. Wind Eng. Ind. Aerod*., 151, 25-36. https://doi.org/10.1016/j.jweia.2016.01.004.

Baker, C.J. (2010), "The simulation of unsteady aerodynamic cross wind forces on trains", *J. Wind Eng. Ind. Aerod.*, **98**(2), 88-99. https://doi.org/10.1016/j.jweia.2009.09.006.

Bhattacharyya, B. and Dalui, S.K. (2018), "Investigation of mean wind pressures on 'E' plan shaped tall building", *Wind Struct*., **26**(2), 99-114. https://doi.org/10.12989/was.2018.26.2.099.

Bo, L., Yang, Q. and Yang, J. (2016), "Wind characteristics near ground in south-eastern coast area of China based on field measurement", *Geomat Nat Haz Risk.*, **7**, 1-13. https://doi.org/10.1080/19475705.2016.1181459.

Cheng, C.M. and Lu, P.C. (1992), "Wind loads on square Cylinder in homogeneous turbulent flows", *J. Wind Eng. Ind. Aerod.*, **41**(1-3), 739-749. https://doi.org/10.1016/0167-6105(92)90490-2.

Chevula, S., Sanz-Andres, Á. and Franchini, S. (2015), "Estimation of the correction term of pitot tube measurements in unsteady (gusty) flows", *Flow Meas. Instrum.*, **46**, 179-188. https://doi.org/10.1016/j.flowmeasinst.2015.08.011.

Dalgliesh, W.A. (1975), "Comparison of model/full-scale wind pressures on a high-rise building", *J. Wind Eng. Ind. Aerod.*, **1**, 55-66. https://doi.org/10.1016/0167-6105(75)90006-9.

Daniels, S.J., Castro, I.P. and Xie, Z.T. (2013), "Peak loading and surface pressure fluctuations of a tall model building", *J. Wind Eng. Ind. Aerod.*, **120**, 19-28. https://doi.org/10.1016/j.jweia.2013.06.014.

Feng, R., Liu, F., Cai, Q., Yan, G. and Leng, J. (2018), "Field measurements of wind pressure on an open roof during typhoons field measurements of wind pressure on an open roof during typhoons HaiKui and SuLi", *Wind Struct*., **26**(1), 11-24. https://doi.org/10.12989/was.2018.26.1.011.

Fiedler, M., Berg, W., Ammon, C., Loebsin, C., Sanftleben, P., Samer, M., Bobrutzki, K.V., Kiwan, A. and Saha, C.K. (2013), "Air velocity measurements using ultrasonic anemometers in the animal zone of a naturally ventilated dairy barn", *Biosyst. Eng.*, **116**(3), 276-285. https://doi.org/10.1016/j.biosystemseng.2012.10.006.

Guo, P., Wang, D.W. and Li, S.L. (2019), "Transiting test method for galloping of iced conductor using wind generated by a moving vehicle", *Wind Struct*., **28**(3), 155-170. https://doi.org/10.12989/was.2019.28.3.155.

He, X., Li, H., Wang, H., Fang, D. and Liu, M. (2017), "Effects of geometrical parameters on the aerodynamic characteristics of a streamlined flat box girder", *J. Wind Eng. Ind. Aerod.*, **170**, 56-67. https://doi.org/10.1016/j.jweia.2017.08.009.

Huang, J. and Gu, M. (2014). "Tests for blockage effects of fluctuating wind pressure on a rectangular tall buildings in uniform flow", *J. Vib. Shock*, **33**, 28-34.

Kim, Y.C., Lo, Y.L. and Chang, C.H. (2018), "Characteristics of unsteady pressures on slender tall building", *J. Wind Eng. Ind. Aerod.*, **174**, 344-357. https://doi.org/10.1016/j.jweia.2018.01.027.

Lee B.E. (1975), "The effect of turbulence on the surface pressure field of a square prism", *J. Fluid Mech.*, **69**(2), 263-282. https://doi.org/10.1017/S0022112075001437.

Li, S., Liang, J., Zheng, S., Jiang, N., Liu, L. and Guo, P. (2019), "A Novel Test Method for Aerodynamic Coefficient Measurements of Structures Using Wind Generated by a Moving Vehicle", *Exp Techniques.*

Li, S., Wan, R., Wang, D. and Guo, P. (2019), "Effect of end plates on transiting test for measuring the aerodynamic coefficient of structures using wind generated by a moving vehicle", *J. Wind Eng. Ind. Aerod.*, **190**, 273-286.

Li, S.L., Liu, L.L., Wu, H., Jiang, N., Zheng, S.Y. and Guo, P. (2019), "New Test Method of Wind Pressure Coefficient Based on CAARC Standard Model Determined Using Vehicle Driving Wind", *Exp Techniques.* **43**(6), 707-717. https://doi.org/10.1007/s40799-019-00330-2.

Liang, J., Tan, H., Kato, S., Zhen, B. and Takahashi, T. (2011), "Wind tunnel investigation on influence of fluctuating wind direction on cross natural ventilation", *Build. Environ*., **46**(12), 2490-2499. https://doi.org/10.1016/j.buildenv.2011.06.006.

Liu, H., Qu, W. and Li, Q. (2011), "Comparison between wind load by wind tunnel test and in-site measurement of long-span spatial structure", *Wind Struct*., **14**(4), 301-319. https://doi.org/10.12989/was.2011.14.4.301.

Liu, X., Niu, J. and Kwok, K. (2013), "Evaluation of RANS turbulence models for simulating wind-induced mean pressures and dispersions around a complex-shaped high-rise building", *Build. Simul.*, **6**(2), 151-164. https://doi.org/10.1007/s12273-012-0097-0.

Lj.Linić, S., Suzana J.Ocokoljić, G., S.Ristić, S., J.Lučanin, V., S.Kozić, M., P.Rašuo, B. and V.Jegdić, B. (2018), "Boundary-layer transition detection by thermography and numerical method around bionic train model in wind tunnel test", *Therm. Sci*., **22**(2), 1137-1148. http://dx.doi.org/10.2298/TSCI170619302L.

Marta, Z., Gori, G. and Guardone, A. (2016), "Blockage and three-dimensional effects in wind-tunnel testing of ice accretion over wings", *J. Aircraft.*, **54**(2), 1-9. https://doi.org/10.2514/1.C033750.

McAuliffe B.R., Belluz, L. and Belzile, M. (2014), "Measurement of the on-road turbulence environment experienced by heavy duty vehicles", *SAE Int. J. Commercial Vehicles*, **7**, 685-702. https://doi.org/10.4271/2014-01-2451.

McAuliffe, B.R. and Chuang, D. (2016), "Track-Based Aerodynamic Testing of a Heavy-Duty Vehicle: Coast-Down Measurements", *SAE Int. J. Commercial Vehicles.*, **9**(2), 381-396. https://doi.org/10.4271/2016-01-8152.

Melbourne, W. H. (1980), "Comparison of measurements on the CAARC standard tall building model in simulated model wind

flows", *J. Wind Eng. Ind. Aerod.*, **6**(1-2), 73-88. https://doi.org/10.1016/0167-6105(80)90023-9.

Meng, F.Q., He, B.J., Zhu, J., Zhao, D.X., Darko, A. and Zhao, Z.Q. (2018), "Sensitivity analysis of wind pressure coefficients on CAARC standard tall buildings in CFD simulations", *J. Build. Eng.*, **16**, 146-158. https://doi.org/10.1016/j.jobe.2018.01.004.

Montazeri, H. and Blocken, B. (2013), "CFD simulation of wind-induced pressure coefficients on buildings with and without balconies: Validation and sensitivity analysis", *Build. Environ.*, **60**, 137-149. https://doi.org/10.1016/j.buildenv.2012.11.012.

Ocokoljić, G., B. Rašuo, B. and Kozić, M. (2017), "Supporting system interference on aerodynamic characteristics of an aircraft model in a low-speed wind tunnel", *Aerosp. Sci. Tech.*, **64**, 133-146. https://doi.org/10.1016/j.ast.2017.01.021.

Ocokoljić, G., Damljanović, D., Vuković, Đ. and Rašuo, B. (2018), "Contemporary frame of measurement and assessment of wind-tunnel flow quality in a low-speed facility", *FME Transactions.*, **46**(4), 429-442. https://doi.org/10.5937/fmet1804429O.

Páscoa, J.C., Brójo, F.P., Santos, F.C. and Fael, P.O. (2012), "An innovative experimental on-road testing method and its demonstration on a prototype vehicle", *J. Mech. Sci. Technol.*, **26**(6), 1663-1670. https://doi.org/10.1007/s12206-012-0413-8.

Rašuo, B. (2001), "On sidewall boundary layer effects in two-dimensional subsonic and transonic wind tunnels", *Zeitschrift fur Angewandte Mathematik und Mechanik.*, **81**, 935-936.

Rašuo, B. (2006), "On boundary layer control in two-dimensional transonic wind tunnel testing", *IUTAM Symposium on One Hundred Years of Boundary Layer Research*., **129**, 473-482. https://doi.org/10.1007/978-1-4020-4150-1_46.

Rašuo, B. (2006), "On Status of Wind Tunnel Wall Correction", *Proceedings of the 25th ICAS Congress*, Hamburg, Germany, September.

Rašuo, B. (2011), "The influence of Reynolds and Mach numbers on two-dimensional wind-tunnel testing: An experience", *The Aeronaut J.*, **115**(1166), 249-254. https://doi.org/10.1017/S0001924000005704.

Rašuo, B. (2012), "Scaling between Wind Tunnels–Results Accuracy in Two-Dimensional Testing", *T. Jpn. Soc. Aeronaut. S.*, **55**(2), 109-115. https://doi.org/10.2322/tjsass.55.109.

Rizzo, F. and Ricciardelli, F. (2017), "Design pressure coefficients for circular and elliptical plan structures with hyperbolic paraboloid roof", *Eng Struct.*, **139**, 153-169. https://doi.org/10.1016/j.engstruct.2017.02.035.

Van Overbeke, P., De Vogeleer, G., Brusselman, E., Pieters, J.G. and Demeyer, P. (2015), "Development of a reference method for airflow rate measurements through rectangular vents towards application in naturally ventilated animal houses: part 3: application in a test facility in the open", *Comput. Electron. Agr.*, **115,** 97-107. https://doi.org/10.1016/j.compag.2015.05.009.

Wang, B., Li, Y., Yu, H. and Liao, H. (2017), "Dynamic reliability evaluation of road vehicle subjected to turbulent crosswinds based on monte carlo simulation", *Shock Vib.*, **2017**, 1-12. https://doi.org/10.1155/2017/2365812.

Wang, H., Mao, J. X. and Spencer Jr, B. F. (2019), "A monitoring-based approach for evaluating dynamic responses of riding vehicle on long-span bridge under strong winds", *Eng. Struct.*, **189**, 35-47. https://doi.org/10.1016/j.engstruct.2019.03.075.

Wang, Y. and Li, Q.S. (2015), "Wind pressure characteristics of a low-rise building with various openings on a roof corner", *Wind Struct.*, **21**(1), 1-23. http://dx.doi.org/10.12989/was.2015.21.1.001.

Wordley, S. and Saunders, J. (2008), "On-road turbulence", *SAE Int. J. Passeng. Cars - Mech. Syst.* **1**(1), 341-360. https://doi.org/10.4271/2008-01-0475.

Wu H. (2018), "Transiting test method to measure wind pressure coefficients of CAARC standard model using wind generated by a moving vehicle", Master Dissertation, Zhengzhou university, Zhengzhou, China.

Yan, B.W. and Li, Q.S. (2015), "Inflow turbulence generation methods with large eddy simulation for wind effects on tall buildings", *Comput. Fluids*, **116**, 158-175. https://doi.org/10.1016/j.compfluid.2015.04.020.

Yi, J. and Li, Q.S. (2015), "Wind tunnel and full-scale study of wind effects on a super-tall building", *J. Fluids Struct.*, **58**, 236-253. https://doi.org/10.10r16/j.jfluidstructs.2015.08.005.

Yu, M., Liu, J., Liu, D., Chen, H. and Zhang, J. (2016), "Investigation of aerodynamic effects on the high-speed train exposed to longitudinal and lateral wind velocities." *J. Fluids Struct.*, **61**, 347-361. https://doi.org/10.1016/j.jfluidstructs.2015.12.005.

Yu, X.F., Xie, Z.N., Zhu, J.B. and Gu, M. (2015), "Interference effects on wind pressure distribution between two high-rise buildings", *J. Wind Eng. Ind. Aerod.*, **142**, 188-197. https://doi.org/10.1016/j.jweia.2015.04.008.

Yuan, C.S. (2011), "The effect of building shape modification on wind pressure differences for cross-ventilation of a low-rise building", *Int. J. Ventilation*, **6**(2), 167-176. https://doi.org/10.1080/14733315.2007.11683775.

Yuan, W.B., Yu, N.T. and Wang, Z. (2018), "The effects of grooves on wind characteristics of tall cylinder buildings", *Wind Struct.*, **26**(2), 89-98. https://doi.org/10.12989/was.2018.26.2.089.

Zhang, J. W. and Q. S. Li. (2018), "Field measurements of wind pressures on a 600m high skyscraper during a landfall typhoon and comparison with wind tunnel test." *J. Wind Eng. Ind. Aerod.*, **175**, 391-407. https://doi.org/10.1016/j.jweia.2018.02.012.

Zhang, J. W. and Q. S. Li. (2018), "Field measurements of wind pressures on a 600m high skyscraper during a landfall typhoon and comparison with wind tunnel test", *J. Wind Eng. Ind. Aerod.*, **175**, 391-407. https://doi.org/10.1016/j.jweia.2018.02.012.

Zhang, J. W. and Li, Q. S. (2018), "Field measurements of wind pressures on a 600 m high skyscraper during a landfall typhoon and comparison with wind tunnel test", *J. Wind Eng. Ind. Aerod.*, **175**, 391-407. https://doi.org/10.1016/j.jweia.2018.02.012.

Zhang, X.l. and Liu P.F. (2017), "Virtual test system for coast-down resistance of motor vehicle with compensation of wind speed and direction", *Transac. Chinese Soc. Agricul. Mach*, **48**, 390-397.

Zou, Q., Li, Z., Wu, H., Kuang, R. and Hui, Y. (2015), "Wind pressure distribution on trough concentrator and fluctuating wind pressure characteristics", *Sol Energy.*, **120,** 464-478. https://doi.org/10.1016/j.solener.2015.02.014.

CC